Theoretical study of signal and geometrical properties of Two-dimensional UWB-based Indoor Positioning Systems using TDoA

Paolo Grasso
Autonomous Vehicles & Artificial Intelligence Laboratory
Research Institute for Future Transport and Cities
Coventry University
Coventry, UK
grassop@coventry.ac.uk

Mauro Sebastián Innocente
Autonomous Vehicles & Artificial Intelligence Laboratory
Research Institute for Future Transport and Cities
Coventry University
Coventry, UK
Mauro.S.Innocente@coventry.ac.uk

***Abstract*—This paper presents an introductory yet comprehensive study of the combined signal and geometrical properties of Indoor Positioning Systems (IPSs) based on ultra-wideband (UWB) technology. These IPSs consist of a network of more than three transmitting anchors and a (tagged) single receiving object to be localised. The specific algorithm used in this paper is the Time Difference of Arrival (TDoA) with round-robin scheduling. The analysis is structured in a systematic manner in order to lay the foundations for the optimal number, location and orientation of anchors aiming for maximum precision, and also for maximum size of the working area with a desired prescribed precision.**

***Index Terms*—UWB, IPS, indoor positioning systems, precision, CRLB, TDoA, geometry, optimal layout.**

I. Introduction

Positioning systems comprise a significant enabling technology in robotics and automation. There are numerous available systems in the market which use a myriad of algorithms and different forms of energy (e.g. electromagnetic or sound waves), each with its own set of strengths and weaknesses. For instance, the Global Positioning System (GPS) is appropriate for efficient outdoor positioning but tends to fail in indoor spaces because radio waves cannot penetrate obstacles. Conversely, ultra-wideband (UWB) technology is short-range and inadequate for outdoor positioning, whilst it presents critical advantages for Indoor Positioning Systems (IPSs) such as high-accuracy and the ability to pass through walls, equipment and other obstacles [1]. In fact, UWB is one of the most recent, accurate and promising technologies for IPSs [2]. Given the task of evaluating the position of a node within a restricted indoor space and in real-time, UWB-based systems are widely considered to be the best choice [1]. Nonetheless, a couple of disadvantages worth mentioning are their high cost and their susceptibility to interference caused by metallic materials and by systems working on similar frequencies.

In this paper, the task of the IPSs is to localise a moving object (a node or drone) based on a spatial distribution of transceivers (anchors) using the Time Difference of Arrival (TDoA) algorithm. The problem of planar source localization in a homogeneous medium with negligible interferences or reverberation is addressed. The traditional way to study the precision of these systems is performing a Cramér–Rao Lower Bound (CRLB) analysis from the signal perspective and then applying coefficients such as Geometric Dilution of Precision (GDOP) in order to capture the geometrical features. CRLB is widely accepted for systems where the node to be localised is far away from the anchors – e.g. in GPS systems – but fails for IPSs [3], [4]. In line with this concerns, we propose a preliminary but rigorous analysis based on [3]–[7] which is expected to enable the optimization of the positioning of the anchors so as to achieve robustness against noise and measuring errors; to perform a statistical analysis of error propagation in TDoA-based positioning systems; and to approach more complex problems accounting for uncertainties in sensor synchronisation and/or sensor placements. An example is the geometrical-statistical approach to remove outliers [8], which shows the strength of this rigorous mathematical approach [3].

Thus, a comprehensive study of combined signal and geometry features of an IPS with a generic number of anchors using round-robin TDoA scheduling is presented, with the purpose of enabling a future optimisation algorithm to seek the optimal distribution and orientation of antennas in a three-dimensional environment. Potential objectives are maximising the precision of the system within the convex hull delimited by the anchors, and maximising the working area with a desired prescribed precision.

The remainder of this paper is organised as follows: in section II, UWB-based IPSs that use the TDoA algorithm are analysed from both the signal and the geometrical perspectives (sections II-A and II-B, respectively); section II-C provides an example of a simple optimisation problem formulated based on the presented analysis of the TDoA-based system, where the objective is to find the maximum square inscribed in the flyable area spanned between four anchors; finally, conclusions are outlined in section III.

P. Grasso & M.S. Innocente, *Theoretical study of signal and geometrical properties of two-dimensional UWB-based indoor positioning systems using TDoA*, In Proceedings of the 6th International Conference on Mechatronics and Robotics Engineering, IEEE, 2020.
DOI: 10.1109/ICMRE49073.2020.9065121

II. Analysis of TDoA-based system

In the following analysis the object to be localised is behaving as a receiver (RX) and all the other anchors as transmitters (TXs) – i.e. source of sound or electromagnetic waves. The reference studies [3]–[7] are still valid even if the object to be localised is treated as TX. This analogy stands as far as the RXs are very sensitive and approximately omnidirectional.

Therefore, according to the usual TDoA studies, the pseudoranges – i.e. range differences – for a localisation system based on only three anchors are:

$$\tau_{ij}(\mathbf{x}) = d_{\mathrm{j}}(\mathbf{x}) - d_{\mathrm{i}}(\mathbf{x}), \quad i,j = 1,2,3 \tag{1}$$

where d_i is the distance between the drone ($\mathbf{x}$) and the ith anchor position ($\mathbf{x}_i$). As suggested in [3], the speed of propagation in the medium is considered to be 1 without loss of generality. The τ_{ij} can be assembled together by defining a TDoA mapping that transforms from the two-dimensional space of source location to a space of pseudoranges called τ-plane, as suggested in [8]:

$$\begin{array}{rccc} \boldsymbol{\tau_2}: & \mathbb{R}^2 & \rightarrow & \mathbb{R}^2 \\ & \mathbf{x} & \rightarrow & (\tau_{12}(\mathbf{x}), \tau_{13}(\mathbf{x})) \end{array} \tag{2}$$

Studying the TDoA map is crucial for the mathematical characterisation of the localisation problem at hand. Considering an IPS that consists of a network of N anchors and one node, M measurements (number that depends on the localisation algorithm) are performed every time step, accordingly to the frequency at which messages are sent from anchors to node. Every measurement is modeled as a normal distribution which is a function of both the real measurements and an additive Gaussian noise, which standard deviation changes in space with the distance from any transmitting anchor. The collection of M measured pseudoranges, $\hat{\boldsymbol{\tau}}^{(k)}$, can be expressed as:

$$\begin{gathered} \hat{\boldsymbol{\tau}}^{(k)} \in \mathbb{R}^M, \\ \hat{\tau}_{ij} \sim \boldsymbol{\mathcal{N}}\left(\tau_{ij}(x), \bar{\sigma}_{ij}^2\right), \quad \bar{\sigma}_{ij} = f(\sigma_i, \sigma_j), \\ \tau_{ij} = \|\mathbf{x} - \mathbf{x}_i\| - \|\mathbf{x} - \mathbf{x}_j\|, \\ i,j \in \{1,\ldots,N\} \quad \text{with} \quad i \neq j, \end{gathered} \tag{3}$$

where $\hat{\tau}_{ij}$ is the individual pseudorange measurement (considering the two times-of-arrival to the node from the ith and jth anchors) and τ_{ij} is the real range difference, and the superscript $^{(k)}$ is the considered time step (to be omitted but implicit in further analyses). Please note that $\hat{\boldsymbol{\tau}}$ is a column vector, not a matrix. The $\hat{\tau}_{ij}$ components can be as many as the binomial coefficient $\binom{N}{3} = \frac{N!}{3!(N-3)!}$.

A. Signal properties

In this section the CRLB analysis for TDoA based IPSs is presented, specifically for round-robin scheduling (subscript $_{rr}$) which, for N anchors, relies on a TDoA measurements set of the form $\boldsymbol{\tau}_{rr} = \{\tau_{12}, \tau_{23}, ..., \tau_{N1}\}$.

The elements of the total Fisher Information Matrix (FIM) for the general positioning problem according to [6], [9] are:

$$\begin{aligned} \mathrm{FIM}_{ij} = &\left(\frac{\partial \boldsymbol{\tau}(\mathbf{x})}{\partial x_i}\right)^{\mathrm{T}} \mathbf{F}_\tau^{-1}(\mathbf{x}) \left(\frac{\partial \boldsymbol{\tau}(\mathbf{x})}{\partial x_j}\right) \\ &+ \frac{1}{2} tr\left(\mathbf{F}_\tau^{-1}(\mathbf{x}) \frac{\partial \mathbf{F}_\tau(\mathbf{x})}{\partial x_i} \mathbf{F}_\tau^{-1}(\mathbf{x}) \frac{\partial \mathbf{F}_\tau(\mathbf{x})}{\partial x_j}\right) \end{aligned} \tag{4}$$

where $\mathbf{F}_\tau$ is the covariance matrix of the $\hat{\boldsymbol{\tau}}$ measurements, and $tr(\mathrm{M})$ is the trace of a matrix M. Since each standard deviation is considered to be changing in space – i.e. $\sigma_i(x,y)$ – the correction term (second row in (4)) is acknowledged in the following analysis.

1) CRLB for round-robin scheduling: The information matrix of the considered TDoA measurements set $\boldsymbol{\tau}_{rr} = \{\tau_{12}, \tau_{23}, \tau_{34}, \tau_{41}\}$ (round-robin scheduling) in the case of four coplanar anchors, using an efficient unbiased estimator, shall be the covariance matrix:

$$\mathbf{F}_\tau = \begin{bmatrix} s_1+s_2 & -s_2 & \mathrm{F}_{13} & -s_1 \\ -s_2 & s_2+s_3 & -s_2 & \mathrm{F}_{42} \\ \mathrm{F}_{31} & -s_3 & s_3+s_4 & -s_4 \\ -s_1 & \mathrm{F}_{42} & -s_2 & s_4+s_1 \end{bmatrix}_{4\times 4} \tag{5}$$

with

$$\begin{aligned} \mathrm{F}_{13} = \mathrm{F}_{31} &= -\sqrt{(s_1+s_2)(s_3+s_4)} \\ \mathrm{F}_{24} = \mathrm{F}_{42} &= -\sqrt{(s_2+s_3)(s_4+s_1)}. \end{aligned}$$

where $s_i = \sigma_i^2$. The elements F_{13}, F_{24} and symmetric ones have been evaluated by manipulating the Cauchy-Bunyakovsky-Schwarz inequality on the expected value of the product of two random variables – i.e. if X and Y are the random variables, $(E[XY])^2 \leqslant E[X^2] \cdot E[Y^2]$. Moreover, the presence of negative correlation between different TDoA measurements in the covariance matrix is specific of the round-robbin scheduling. For instance, if the TDoA algorithm was centred with respect to *anchor 1*, all the values, except the main diagonal, would be equal to $+s_1$ as shown in [6], [7], [10].

Studies, such as [6], state that the lower bound of the squared standard deviation of the TOA measurements due to an additive Gaussian white noise is bounded by:

$$\sigma^2 \geqslant \frac{c^2}{\mathrm{SNR} \cdot B_{\mathrm{w}}^2} \tag{6}$$

where SNR is the signal-to-noise ratio, c is the speed of light, and B_{w} is the bandwidth of the considered channel.

While [6] proposes a quadratic relationship with the distance from the source with a C^0 continuity, a more rigorous formulation is considered in the presented analysis.

The SNR in (7) is the ratio between the power of the signal reaching the receiver (P_{r}) and the noise power (P_{N}). It can be written as function of the distance (d) between transmitter ($_t$) and receiver ($_r$), the representative transmission frequency (f_{ref}) and bandwidth of the selected channel, the temperature of the environment (T), the transmitting power (P_{t}) and the gain of the transmitting antenna (G_{t}) and receiving antenna. While the latter can be neglected in this analysis (since usually

the receiving antenna is very sensitive), the gain G_{t} can be a function of the azimuth (θ_{t}) and elevation (ϕ_{t}) angles with respect to the frame of reference centred on the antenna.

$$\mathrm{SNR}\left(d, \theta_{\mathrm{t}}, \phi_{\mathrm{t}}, f_{\mathrm{ref}}, T, P_{\mathrm{t}}\right) = \frac{P_{\mathrm{r}}}{P_{\mathrm{N}}} \tag{7}$$

The power at the end of the transmission line can be expressed using the contemporary Friis law shown in (8).

$$P_{\mathrm{r}} = \frac{P_{\mathrm{t}} \cdot G_{\mathrm{t}} \cdot G_{\mathrm{r}}}{L_{\mathrm{t}} \cdot L_{\mathrm{r}}} \cdot \left(\frac{c}{4\pi \cdot f_{\mathrm{ref}} \cdot d}\right)^2 \tag{8}$$

where L_{t} and L_{r} are the electric losses in the electronics of the TX and RX modules, respectively. These have been embedded in the gains G_{t} and G_{r}.

It is convenient to express everything in logarithmic form. Note that the unit [dBm] stands for 'dB milli-watts'. Combining (8) and (6), one could obtain the upper bound of the standard deviation, as expressed in the system in (9). Note that the noise power is expanded as thermal noise power term, $\mathrm{k_B} T B_{\mathrm{w}}$.

$$\begin{cases} \mathrm{SNR}_{\mathrm{dB}} = P_{\mathrm{tdBm}}(T, V_i) + G_{\mathrm{tdBi}}(\theta_{\mathrm{t}}, \phi_{\mathrm{t}}) \\ -10\log_{10}(\mathrm{k_B} T B_{\mathrm{w}} 10^3) - 20\log_{10}\left(4\pi f_{\mathrm{ref}} d/c\right) \\ \sigma^2 = \frac{c^2}{B_{\mathrm{w}}^2} \cdot 10^{-\mathrm{SNR}_{\mathrm{dB}}/10} \end{cases} \tag{9}$$

where $P_{\mathrm{tdBm}}(T, V_i)$ is an experimental curve approximating the relation of the transmission power with the ambient temperature and the input voltage (V_i) [11], and $G_{\mathrm{tdBi}}(\theta_{\mathrm{t}}, \phi_{\mathrm{t}})$ is the measured transmitting antenna gain (with respect to an isotropic antenna 'i'), which is a three-dimensional radiation pattern function of the azimuth and elevation angles [12]. The presented CRLB analysis has been applied for two different distributions of four anchors: a symmetric positioning and a random one, as shown in Figure 1.

B. Geometrical properties

In this section, geometrical issues intrinsic to the underlying mathematics of the TDoA algorithm are analysed according to [3]. For instance, a known problem of IPSs that has geometrical origin is the *flipping uncertainty*, as shown in [4]. In the following sections, the *flyable area* is defined based on the combination of the previous CRLB analysis and the envelope of the bifurcation curves, which define the limits of the used localisation algorithm.

1) Bifurcation Curve: The bifurcation curve is the projection of the TDoA map boundaries from the τ-plane (pseudorange space) to the 2D (or 3D) space of source location. The bifurcation curve, as defined in [3], is the quintic curve $\tilde{E}(\mathbf{x})$ depicted by the roots of a polynomial $P(\mathbf{x})$ which is the representation of the TDoA map constraints. The definition of $P(\mathbf{x})$ and some examples of algebraic equations of $\tilde{E}(\mathbf{x})$ can be found in [5], whilst its rigorous derivation is explained in [3], using tools like exterior algebra formalism and Minkowski space. This formulation is invariant under permutation of the TDoA measurements, hence the scheduling does not affect this

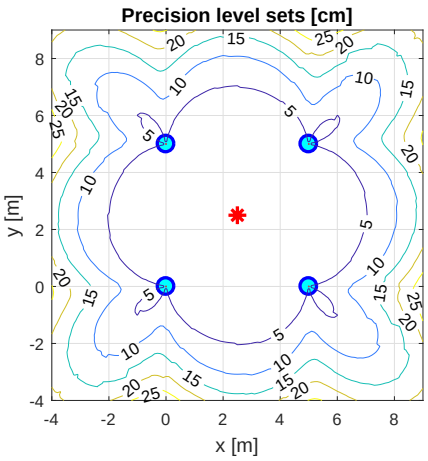

(a) Symmetric anchors' positioning

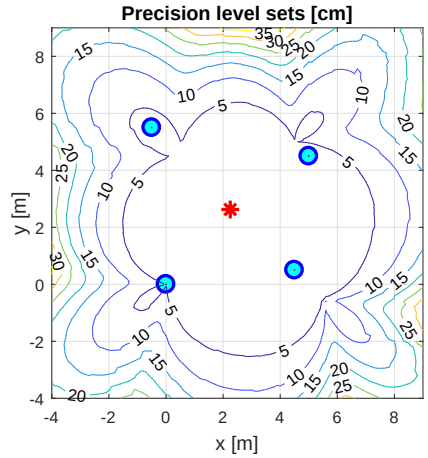

(b) Random anchors' positioning

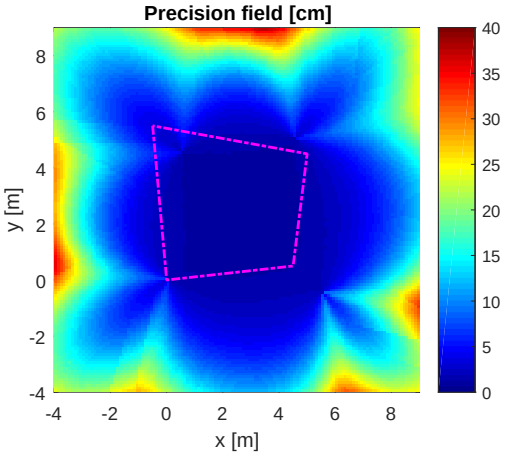

(c) Random anchors' positioning

Fig. 1: Precision level sets for two cases, (a) and (b). The best precision (in this case about ± 5 cm with 99% confidence level - i.e. k = 2.58) is obtained in the convex hull delimited by the anchors. A realistic non-isotropic TX-antenna gain (DWM1000 module [12]) is also applied for the estimation of the SNR, hence the slight fluctuations in the represented values. In (c), the precision field is shown only for the random case; the convex hull is the dotted magenta trapezoid.

analysis. Any TDoA-based localisation system has a unique solution of the positioning problem if $P(\mathbf{x})$ is negative – i.e. le localisation region between the bifurcation curves surrounding the anchors. The TDoA maths within the bifurcation curves gives either two mirrored solutions, which cannot be distinguished, or complex solutions, which have no physical sense. An example of bifurcation curves is shown in Figure 2(a) for the set of only three anchors $\{m_2, m_3, m_4\}$

2) Bifurcation Envelope & Flyable Area: As explained in the previous section, the concave regions of the bifurcation curves are places where the position of the vehicle cannot be measured. Hence, being strictly conservative, there is the need of finding the maximum envelope of all the triplets of bifurcation curves on each node. Here this curve is called bifurcation envelope and it is represented by Ω. In Figure 2(b,c) the *flyable area* (in yellow) is defined as the intersection of two areas: the unique-solution area enclosed by the envelope of the bifurcation curves (in green) and the acceptable-precision region, which is the outcome of the previous CRLB analysis.

C. Towards an optimisation of anchors' positioning

The introductory rigorous analysis presented in the previous sections sets the foundation for enabling the optimisation of the positioning of the antennae within an available space. For example in a three-dimensional experiment's environment, an optimisation problem could consist of finding the maximum cube inscribed in a convex flyable hull while also maximising the precision of the localisation of a drone. For instance, the explanatory optimisation problem shown in Figure 3 aims to find the centroid (x_c^*, y_c^*) of the maximum square inscribed in the polygon bounded by the envelope of the bifurcation curves, Ω, and the hull delimited by the antennae. This nested optimisation problem, depicted in Figure 4, has as its inner level an 'inflation problem' (Opt.2). The solutions for the two cases considered in the previous CRLB and geometrical studies are shown in Figure 3.

III. Conclusions

A theoretical study of the signal properties and an analysis of the geometrical limit of an Indoor Positioning System (IPS) was presented based on the Time Difference of Arrival (TDoA) algorithm with round-robin scheduling. This comprehensive analysis is critical for the formulation of the optimal IPS design. In its simplest form, this may be aimed at the best layout of the anchors in terms of spatial locations and orientations to maximise the system's precision. An initial example was formulated and solved, consisting of finding the maximum square area inscribed in a polytope that encloses the region where localisation is defined - e.g. flyable area.

At present, this work is being extended towards a more comprehensive formulation of the optimal design problem, which may be defined as follows: given the position of one anchor comprising the origin of the frame of reference, find the optimal position of the remaining anchors in order to obtain the maximum flyable region with the prescribed acceptable precision. In addition, we are currently building

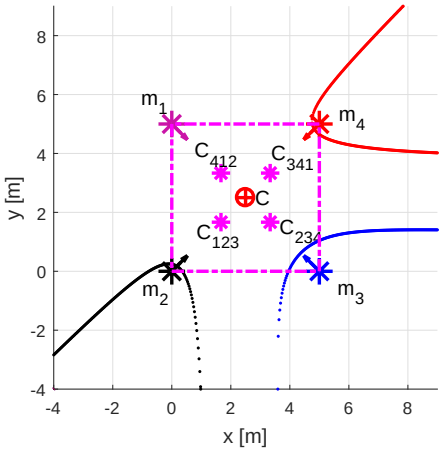

(a) Symmetric anchors' positioning

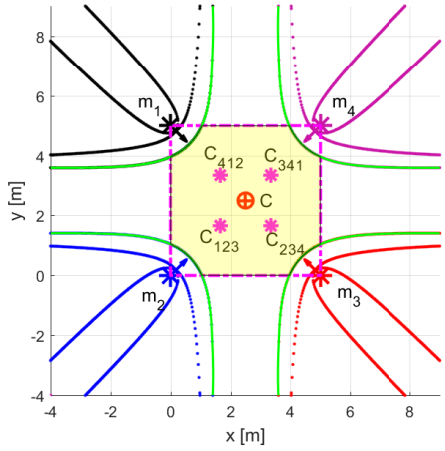

(b) Symmetric anchors' positioning

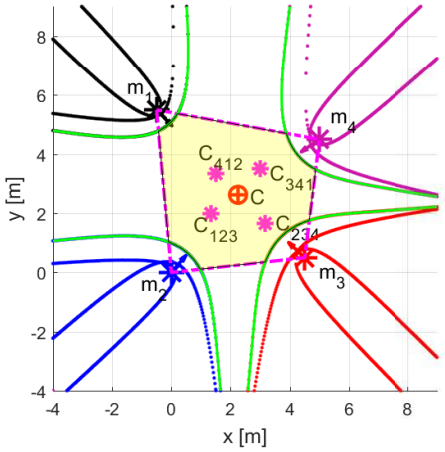

(c) Random anchors' positioning

Fig. 2: In (a), three distinctly highlighted root loci representing the bifurcation curves around three anchors for the selected couple of TDoA measurements τ_{23} and τ_{34}. The points m_i for $i = 1, \ldots, 4$ are the assigned positions of the transmitting anchors, C_{ijk} are the centroids of the considered triplet, and C is the collective centroid. In (b) and (c), the *flyable area* is highlighted in yellow, the envelope of the bifurcation curves is the continuous green curve, and the convex hull with acceptable-precision is the dotted magenta trapezoid.

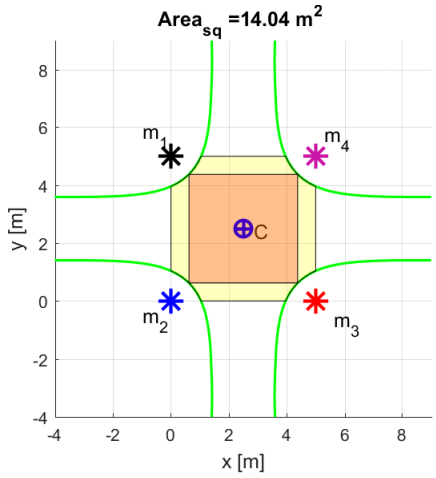

(a) Symmetric anchors' positioning

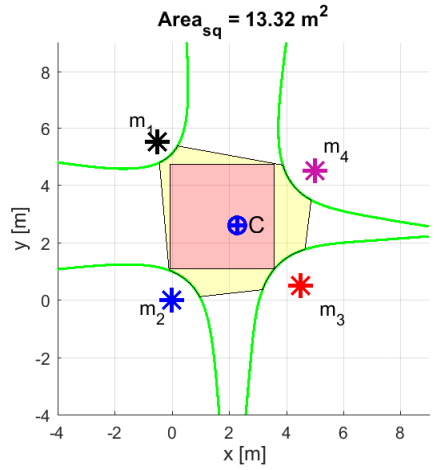

(b) Random anchors' positioning

Fig. 3: Some solutions of the maximum square inscribed in the flyable areas depicted in Figure 2. In this numerical example in (b) the square is 1 m^2 smaller than in the (a) symmetric case.

Opt.1		Find centroid of the maximum inscribed square: $\min_{x_c, y_c} \{-f(x_c, y_c)\}$ gives the optimal solution (x_c^*, y_c^*)
	Opt.2	Find largest inscribed square for a given centroid $(\mathrm{x_c}, \mathrm{y_c})$: $\min_{L} \{-L^2 + \mathrm{c} \cdot A_{\text{out}}(\mathrm{x_c}, \mathrm{y_c}, L)\}$ gives the optimal solution L^* $f(x_c, y_c) = L^{*2}, \quad \mathrm{c} \approx 10^6$

Fig. 4: Algorithm formulated for the optimisation problem of finding the maximum square inscribed in Ω. L is the edge of the square, and A_{out} is the area of the region, of the attempted square, that is outside Ω.

an experimental platform for tests and validation of these and future theoretical developments. In the future, this will also be used as a positioning system for indoor experiments to test self-coordination and multi-agent collision-avoidance algorithms (e.g. in [13]).

References

[1] A. Alarifi, A. Al-Salman, M. Alsaleh, A. Alnafessah, S. Al-Hadhrami, M. Al-Ammar, and H. Al-Khalifa, "Ultra wideband indoor positioning technologies: Analysis and recent advances," *Sensors*, vol. 16, no. 5, p. 707, may 2016.

[2] M. Ghavami, L. Michael, and R. Kohno, *Ultra Wideband Signals and Systems in Communication Engineering*. John Wiley & Sons, 2007.

[3] M. Compagnoni, R. Notari, F. Antonacci, and A. Sarti, "A comprehensive analysis of the geometry of TDOA maps in localization problems," *Inverse Problems*, vol. 30, no. 3, p. 035004, feb 2014.

[4] S. O. Dulman, A. Baggio, P. J. Havinga, and K. G. Langendoen, "A geometrical perspective on localization," in *Proceedings of the first ACM international workshop on Mobile entity localization and tracking in GPS*. ACM Press, 2008.

[5] M. Compagnoni and R. Notari, "Tdoa-based localization in two dimensions: the bifurcation curve," *Fundamenta Informaticae*, vol. 135, no. 1-2, pp. 199–210, 2014.

[6] R. Kaune, J. Horst, and W. Koch, "Accuracy analysis for tdoa localization in sensor networks," in *14th International Conference on Information Fusion*, 2011.

[7] R. Kaune, "Accuracy studies for tdoa and toa localization," Aug. 2012.

[8] M. Compagnoni, A. Pini, A. Canclini, P. Bestagini, F. Antonacci, S. Tubaro, and A. Sarti, "A geometrical–statistical approach to outlier removal for TDOA measurements," *IEEE Transactions on Signal Processing*, vol. 65, no. 15, pp. 3960–3975, aug 2017.

[9] S. M. Kay, *Fundamentals of Statistical Processing, Volume I*. Prentice Hall, 1993.

[10] T. Sathyan, M. Hedley, and M. Mallick, "An analysis of the error characteristics of two time of arrival localization techniques," in *2010 13th International Conference on Information Fusion*. IEEE, jul 2010.

[11] Decawave-Ltd, "Dw1000 datasheet v2.09," 2015.

[12] Decawave-Ltd., "Dwm1000 datasheet v1.3," 2015.

[13] M. S. Innocente and P. Grasso, "Self-organising swarms of firefighting drones: Harnessing the power of collective intelligence in decentralised multi-robot systems," *Journal of Computational Science*, vol. 34, pp. 80–101, may 2019.